

# Enhanced High Activity for Removal and Adsorption Process of Cationic Dye by Using Active Nanocomposite Surface: Reactivation and Isotherm Models

Aseel M. Aljeboree\* and Ayad F. Alkaim

Department of Chemistry, College of Science for Women, University of Babylon, Babylon, Iraq

✉ annenayad@gmail.com

*Received July 11, 2023; revised and accepted August 4, 2023*

**Abstract:** In this research, a new low-cost material was synthesised multi carbon nanotube/Zinc oxide nanocomposite (MWCNT/ZnO), nanocomposite used as a sorbent for dye removal from industrial Water treatment, as like cationic model Maxillon blue (GRL) dye in order to find the adsorption mechanism of adsorption methods were studied via FESEM, TEM, and BET. Two models of Freundlich and Langmuir isotherm were studied, and according to the data, it was established that it conforms to the isotherm Freundlich estimation on the value of  $R^2 > 0.9798$ . The reactivation and re-use of (MWCNT/ZnO) nanocomposite were performed by using water in the GRL dye up to Cycle 5 under the best conditions. After the 3 cycles of using (MWCNT/ZnO) nanocomposite, the efficiency is still significant ( $>80\%$ ) and it appears that the (MWCNT/ZnO) nanocomposite is a probable re-newable absorber, moreover, the effect of ionic strength increases the solubility of the GRL dye in aqueous medium. Thus, when salt is added, the aqueous solution decreases the removal percentage. Also, a comparison among several surfaces (ZnONPs, MWCNT, MWCNT/ZnO), found MWCNT/ZnO nanocomposite the best surfaces to remove GRL dye.

**Key word:** Adsorption, removal, maxillon blue (GRL) dye, isotherm, zinc oxide, nanocomposite.

## Introduction

Multi carbon nanotube (MWCNT) is one of the most important and widely used adsorbents to get rid of toxic organic and inorganic pollutants, dyes, and lasting and toxic phenolic compounds, which is characterised by its advanced porous structure and high surface area that leads to good absorption properties (Farzadkia et al., 2018; Kalantary et al., 2012; Khedaer et al., 2021; Konicki et al., 2012; Wared and Radia, 2021). Depending on these important physical properties, the absorption efficiency also depends on the source of the use of organic materials in the preparation of Multi carbon nanotube, in addition to the investigational

conditions employed in the activation methods. MWCNT can be prepared using a variety of physical and chemical methods (Attia et al., 2008, Taka et al., 2020, Abdulrazzak et al., 2021). Zinc oxide (ZnO) can be set in nature as a zincate mineral; thus, the plurality of it is prepared unnaturally. The structure of crystal found in a hexa-gonalwurt-zite form or cubic zinc blende (Mashkour et al., 2011). Zinc oxide is generally utilised for treating skin-related problems, for example, nappy rash and dandruff and also incorporated in ointments to be utilised in wound dressing (Stefaniuk et al., 2019, Zhang et al., 2019). Where adsorbent MWCNT incorporated with zinc oxide NPs was utilised. Zinc oxide NPs enhanced the recovery of the

\*Corresponding Author

adsorbent from the aqueous water after the elimination of pollutants (Aljeboree et al., 2019; Mashkour et al., 2011).

Maxillon blue (GRL) dye, as shown in Figure 1, and having a molecular formula  $C_{30}H_{26}N_4Na_2O_8S_2$ , is an odourless blue powder utilised for several purposes, e.g., stain biological and dermatological agents, medicine veterinary, and an additive to poultry feed to inhibit propagation of mold, fungus, and intestinal parasites. It is too extensively utilised in paper printing and textile dying (Awad et al., 2019). About 0.7–2 kg of GRL is consumed per ton of paper produced. Although GRL causes gastrointestinal irritation in humans, symptoms include diarrhoea, vomiting, and nausea. It also irritates the respiratory system, causing shortness of breath, and this causes severe coughing continuously. Also, it is dangerous when touching the skin, causing severe irritation and redness of the skin. Maxillon blue (GRL) may form a highly hazardous and highly toxic dye and produce gases like nitrogen oxides, carbon oxides, and sulphur oxides when heated to decompose.

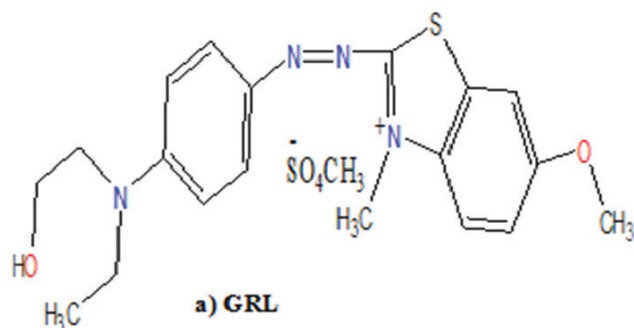


Figure 1: The chemical structure of Maxillon blue (GRL) dye.

This research aims to study the removal of pollutants by using highly active surface and show their activity as reactivation and isotherm models.

### Experimental Part

#### Synthesis of MWCNT/Zinc Oxide Nanocomposite

Multiwall carbon nanotubes (MWCNT) were acquired from incineration chimneys in furnaces in Hilla/Iraq, and treated with concentrated  $H_3PO_4$  (0.1N) with continuous stirring for 2hr, then washed several times with distiller water, filtrated and dried at  $65^\circ C$ . ZnO NPs were prepared in the laboratory via adding 5 g each of oxalic acid and zinc acetate, dissolved in distilled water and mixed for 1h, after that adding of multi carbon

nanotubes 0.1 g and mixed in ultra-sound for 30 min until the mixture became. Then it was processed using a hydrothermal method for 24 hr. at  $160^\circ C$ , and the nanocomposite was washed several times in D.W. and dried at  $70^\circ C$  overnight to get the powder utilised in the experiment.

#### Batch Adsorption Experiments

A standard (GRL) dye solution 1000 mg/L was prepared by dissolving 1.0 g GRL dye in 1000 mL of distiller water. About 100 ml of GRL dye solution (100 mg/L) was taken in an elementary flask of (MWCNT/ZnO) nano-composite (0.05g/100ml) and kept separately at shaker-controlled temperature. The influence of solution pH on the removal of GRL was studied by adjusting the pH solution of GRL to about 3–10.5 at a concentration of 100 mg/L. About 0.1N NaOH and/or HCl were added. After removal of the (MWCNT/ZnO) by filtration by a centrifuge of 2000 rpm, the concentration of dye in the supernatant was determined by a UV-visible spectroscopy. The removal percentage ( $R\%$ ) and adsorption capacity ( $Q_e$ , mg/g) are calculated in Equations 1 and 2.

$$R\% = \frac{C_i - C_e}{C_o} \times 100 \quad (1)$$

$$Q_e = \frac{C_i - C_e}{W} \times V \quad (2)$$

where  $C_i$  initial concentration of dye,  $C_e$  equilibrium conc. mg/L of dye in the solution,  $V$  volume of dye (mL),  $W$ (g) is the mass of (MWCNT/ZnO).

### Results and Discussion

Figure 2a represents carbon nanotubes, where tube-like clusters appeared on the surface interconnected with each other in the form of small channels, and Figure 2b after loading zinc oxide onto carbon nanotubes, where irregular clusters appeared as evidence of zinc oxide loading. Figure 2c represents the nanocomposite after adsorption, where we note that all the active sites are surface packed and clear evidence of loading onto dye within the nanocomposite and the success of the adsorption way. Also, a technique with TEM was used to estimate the characteristics of the synthesis nanocomposite, where it was observed that small tube-like clusters of carbon nanotubes appeared on zinc oxide, and this is evidence of zinc oxide loading on the carbon nanotube as shown in Figure 2d (Abid Alradaa and Kadam, 2021; Bader et al., 2019).

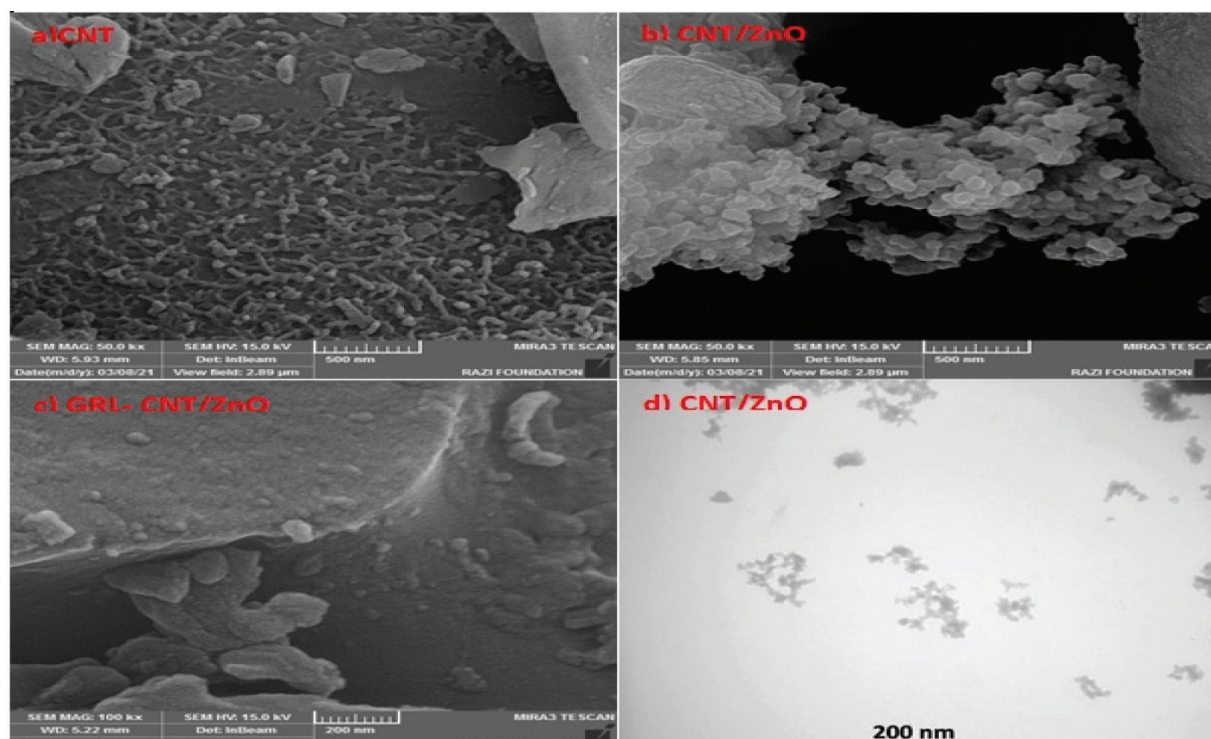


Figure 2: FE-SEM of (a) CNT, (b) ZnO/CNT and (c) GRL dye ZnO/CNT after and before adsorption of GRL dye and (d) TEM CNT/ZnO.

### Surface Area Analyser (BET)

The porosity and surface area of the prepared surface (MWCNT/ZnO) nanocomposite were determined through the use of the BET technique, where this technique depends on the distribution of the pore size of the nanocomposite (Wared and Radia, 2021). This shape was classified as Type IV, and the surface porosity and pore size were improved after incorporating zinc oxide into carbon nanotubes (Radia et al., 2022) as shown in Figure 3.

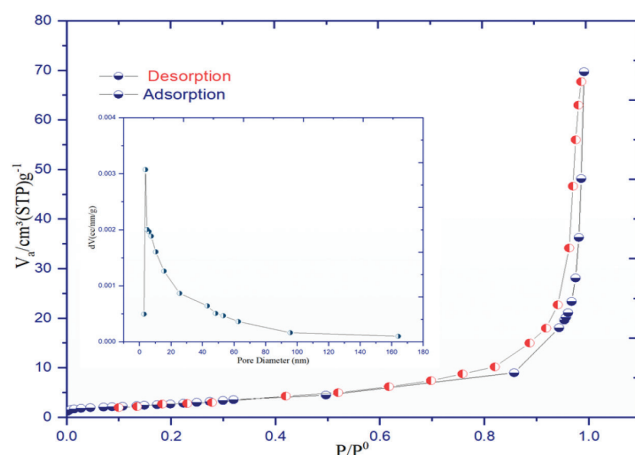


Figure 3: Surface area analyser (BET) of nanocomposite.

### Reactivation of Nanocomposite

The reactivation of (MWCNT/ZnO) nanocomposite, after sorption, is one very economically important parameter for the handling way. It assists in elucidating the mechanism of GRL removal and loading GRL dye of the adsorbent, reactivation mechanism and recycling of adsorbents spent which in turn may decrease operational cost and protect the environment from the secondary dye. The GRL drug desorption studies were carried out utilising water. The performance and reuse of (MWCNT/ZnO) nanocomposite by using water in the GRL dye adsorption way was studied up to step 3 under best conditions. After the 3 cycles of using (MWCNT/ZnO) nanocomposite, the efficiency is still significant (>80%) and this shows that the (MWCNT/ZnO) nanocomposite is probably renewable absorber (Pashaei-Fakhri et al., 2020).

### Comparative Adsorption at Several Surfaces

A comparative was studied among several surfaces (ZnO NPs, MWCNT, MWCNT/ZnO) as that can work as adsorbents. A 100 mL sample of GRL dye concentration ( $100 \text{ mg.L}^{-1}$ ) was added in the presence of 0.1g from several surfaces (ZnO NPs, MWCNT, MWCNT/ZnO) and put in a water bath shaker for 60 min (Radia et al., 2022). The result in Figure 4 reveals

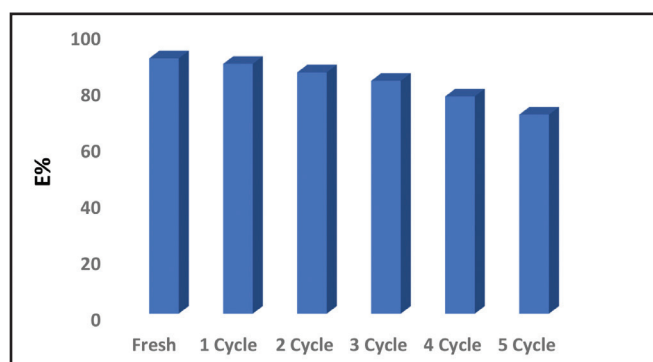


**Figure 4: Number of the reactivation of (MWCNT/ZnO) nanocomposite.**

that the MWCNT/ZnO nanocomposite is the best surface to remove GRL dye.

Comparison of the adsorption of GRL dye onto nanocomposite and other adsorbent material is shown in Table 1.

#### Ionic Strength

Figure 5 shows a decrease in the adsorption efficiency of GRL adsorbed with added salts, and this reduction is due to the effect of competition among molecules

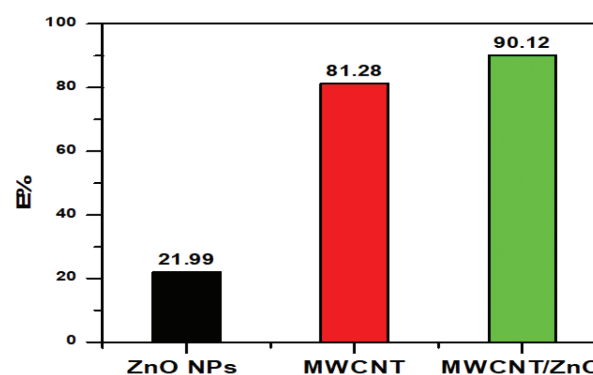


**Figure 5: Effect of comparison between several surfaces.**

of positive GRL and positive ions of salts onto active sites. The existence of the electrolyte in the solution reasons neutralisation of the charged surface of the adsorbent while competing with molecules dye onto the surface. Furthermore, with the rising strength, the ionic adsorption efficiency reduces due to the isolation of the surface charges for molecules dye. Also, the addition of salts give rise to the solubility of the dye in their aqueous medium (Mosaa et al., 2019).

**Table 1: Removal of dyes using different surfaces**

<i>Sorbent</i>	<i>Dyes</i>	<i>T (°C)</i>	<i>pH</i>	<i>t (hr.)</i>	<i>Dose (g.L<sup>-1</sup>)</i>	<i>Q<sub>e</sub> (mg/g)</i>	<i>E%</i>	<i>C<sub>o</sub> (mg.L<sup>-1</sup>)</i>	<i>Ref.</i>
MWCNTs-Fe <sub>3</sub> C	Direct Red 23	30	7	3	0.04	65	–	20	Konicki et al. (2012)
ZnO/AC	Bromophenol red (BPR)	30	5.5	12	0.01	200	97	25	Ghaedi et al. (2013)
ZnO/AC	Bromocresol Green	30	6	1	0.05	57.80	–	20	Ansari et al. (2016)
ZnO/AC	Eosin Y	30	6.6	1	0.05	61.73	–	20	Ansari et al. (2016)
ZnO/AC	Methylene Blue	25	6	1	0.022	89.29	88	8	Dil et al. (2016)
ZnO/AC	Eosin Yellow	25	6	1	0.022	87.52	88.2	9	Dil et al. (2016)
ZnO/AC	Acridine Orange	25	6	1	0.022	88.5	74	10	Dil et al. (2016)
ZnO/AC	Crystal Violet	25	6	1	0.022	93.46	96	8	Dil et al. (2016)
CNT / Fe <sub>3</sub> O <sub>4</sub>	Methylene blue	25	8	1	0.2	248	90	50	Kalantary et al. (2018)
CNTs/ Fe <sub>3</sub> O <sub>4</sub>	Crystal Violet	25	8	24	0.1	287	–	50	Hosseinzadeh et al. (2018)
CNT/Fe <sub>3</sub> O <sub>4</sub>	Methylene blue	25	8	24	0.1	302	–	50	Hosseinzadeh et al. (2018)
CNT/Fe <sub>3</sub> O <sub>4</sub>	Rhodamine B	25	8	24	0.1	231	–	50	)Hosseinzadeh et al. (2018)
zinc oxide	Methylene blue	30	7	2	0.2	115.4	90	100	Somu and Paul (2018)
zinc oxide	Congo red	30	7	3	0.2	62.19	90	50	Somu and Paul (2018)
ZnO	Methylene blue	25	–	1	0.3	74.53	–	70	Shaw et al. (2018)
ZnO/AC	Crystal Violet	20	7	1	0.02	37.49	82.1	50	Karimi et al. (2019)
CNT/Fe <sub>3</sub> O <sub>4</sub>	Methylene blue	25	7	1	0.75	1449	87	200	Zhao Zhan et al. (2020)
CNT/Fe <sub>3</sub> O <sub>4</sub>	Congo red	25	7	1	0.75	1006	83	200	Zhao et al. (2020)



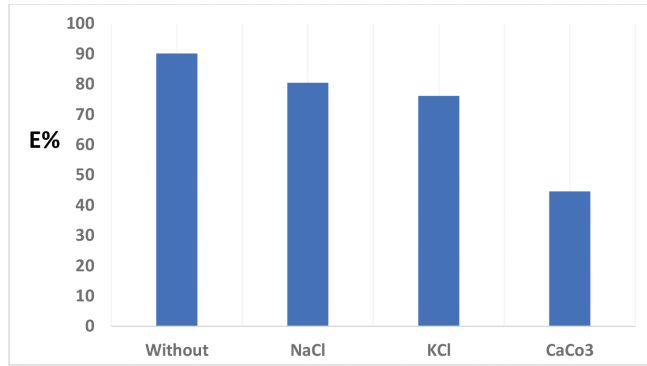


Figure 6: Effect of ionic strength on the adsorption of GRL dye.

### Zero Point Charge

The pH drift way was used for the pH pzc rough calculation. pH pzc is the point where the curve of pH 1 vs. pH 2 crosses the line pH 1 = pH 2, with the composite value being 3 as shown in Figure 6. At pH < pH<sub>pzc</sub>, the composite shows a net charge positive, whilst at pH > pH<sub>pzc</sub> the surface is charged negatively. At basic medium (pH > pH<sub>pzc</sub>), the quantity of OH<sup>-</sup> ion increases in the aqueous medium and the functional groups in the nanocomposite structure have a charge negative which can be active to the removal dyes (Ahlawat et al., 2019).

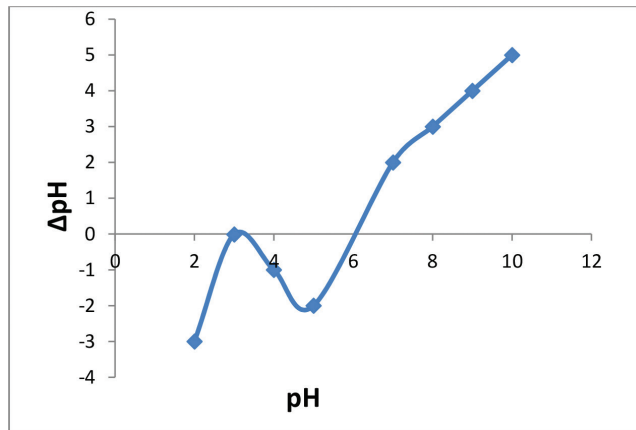


Figure 6: Zero point charge of nanocomposite.

### Adsorption Isotherms

Study two isotherm Freundlich and Langmuir were utilised to define adsorption equilibrium. Isotherm Langmuir theory is based on the assumption of adsorption of the surface homogeneous. The nonlinear model of Langmuir's is represented via an equation (Radia et al., 2022). The non-linear form of the Freundlich isotherm model is given via Equation 3:

$$q_e = K_f C_e^{1/n} \quad (3)$$

The model Langmuir isotherm is commonly utilised for dye adsorption from liquid solutions. The nature of the adsorption process was derived from Langmuir's alternative Equation 4 (Langmuir, 1918).

$$q_e = \frac{q_m K_L C_e}{1 + K_L C_e} \quad (4)$$

$q_e$ : amount adsorbed per unit mass of adsorbent at equilibrium (mg/g),  $C_e$ : equilibrium concentration (mg.L<sup>-1</sup>),  $q_m$ : represents maximum adsorption efficiency (mg/g).  $K_L$ : empirical constant Langmuir (L/mg). The coefficients of estimation ( $R^2$ ) and isotherm model factors from the non-linear regressive way were listed in Tables 1 and 2. A comparison of non-linear fitted curves from experimental result shows two isotherms. Figure 7 shows a plot of  $q_e$  versus  $C_e$ , where the  $K_F$  value and  $1/n$  are found from the intercept and slope of the nonlinear regressions (Aljeboree et al., 2019).

Table 2: The correlation coefficients ( $R^2$ ) and constants of isotherm Langmuir, Freundlich isotherm of adsorption GRL dye adsorbed on to nanocomposite at 20°C

Nanocomposite			
Freundlich	$K_f$	89.627	7.7725±
	1/n	0.3067	0.0319±
	$R^2$	0.96813	
Langmuir	$q_m$ (mg/g)	247.911	32.312±
	$K_L$ (L/mg)	0.418	0.2289±
	$R^2$	0.8295	

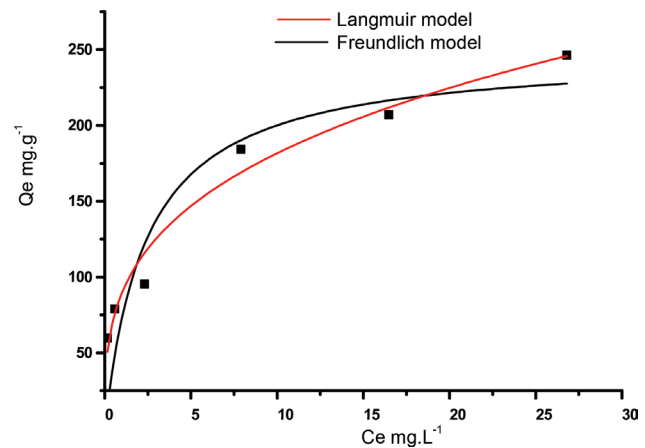


Figure 7: Langmuir isotherm (A), Freundlich isotherm (B), of GRL dye adsorption nanocomposite.

## Conclusion

The highly active nanocomposite surface was prepared by using the hydrothermal method. The main purpose of the process depended on the loading of zinc oxide nanoparticles onto the surface of carbon nanotubes to increase the surface area. Furthermore, the efficiency of the surface in removing the polluted GRL dye from aqueous solution increases, meanwhile, increasing the ability of the surface to reactivate and get utilised more than once and reduce the economic cost, reused and eco-friendly. Results show the adsorption process following the Freundlich model as an adsorption isotherm.

## References

- Abdulrazzak, F.H., Jawad, M.A., Alkadir, O.K.A and A.F. Alkaim (2021). Antimicrobial Activity of Ag:ZnO/MWCNT Against *Cinetobacter baumannii*. *Journal of Nanostructures*, **11(2)**: 317-322.
- Abid Alradaa, Z.A. and Z.M. Kadam (2021). Preparation, characterization and prevention of biological pollution of 4-(4-benzophenylazo) pyrogallol and their metal complexes. *IOP Conference Series: Earth and Environmental Science*, **790(1)**: 012038.
- Abu-Zurayk, R.A., Al Bakain, R.Z., Hamadneh, I. and A.H. Al-Dujaili (2015). Adsorption of Pb(II), Cr(III) and Cr(VI) from aqueous solution by surfactant-modified diatomaceous earth: Equilibrium, kinetic and thermodynamic modeling studies. *International Journal of Mineral Processing*, **140**: 79-87.
- Ahlawat, W., Kataria, N., Dilbaghi, N., Hassan, A.A., Kumar, S. and K.-H. Kim (2019). Carbonaceous nanomaterials as effective and efficient platforms for removal of dyes from aqueous systems. *Environmental Research*, **181**: 108904.
- Al-Bayati, R.A. (2020). Adsorption-desorption isotherm of one of antidiabetic drug from aqueous solutions on some pharmaceutical adsorbents. *Eur. J. Sci. Res.*, **40**: 580-588.
- Aljeboree, A.M., Alshirifi, A.N. and A.F. Alkaim (2019). Removal of pharmaceutical amoxicillin drug by using (Cnt) decorated clay/Fe<sub>2</sub>O<sub>3</sub> micro/nanocomposite as effective adsorbent: Process optimization for ultrasound-assisted adsorption. *International Journal of Pharmaceutical Research*, **11(4)**: 80-86.
- Aljeboree, A.M., Hussein, F.H. and A.F. Alkaim (2019). Removal of textile dye (methylene blue mb) from aqueous solution by activated carbon as a model (corn-cob source waste of plant): As a model of environmental enhancement. *Plant Archives*, **19**: 906-909.
- Ansari, F., Ghaedi, M., Taghdiri, M. and A. Asfaram (2016). Application of ZnO nanorods loaded on activated carbon for ultrasonic assisted dyes removal: Experimental design and derivative spectrophotometry method. *Ultrasonics Sonochemistry*, **33**: 197-209.
- Attia, A.A., Girgis, B.S. and N.A. Fathy (2008). Removal of methylene blue by carbons derived from peach stones by H<sub>3</sub>PO<sub>4</sub> activation: Batch and column studies. *Dyes and Pigments*, **76(1)**: 282-289.
- Awad, H.M., Alkaim, A.F. and M.N. Al-Baiati (2019). Adsorption of maxilon blue (GRL) from aqueous solutions by using a novel nano-composite polymer. *IOP Conference Series: Materials Science and Engineering*, **571**: 012095.
- Bader, A.T., Zaied, A.M., Aljeboree, A.M. and A.F. Alkaim (2019). Removal of methyl violet (MV) from aqueous solutions by adsorption using activated carbon from pine husks (plant waste sources). *Plant Archives*, **19**: 898-901.
- Dil, E.A., Ghaedi, M., Ghaedi, A., Asfaram, A., Goudarzi, A., Hajati, S., Soylak, M., Agarwal, S. and V.K. Gupta (2016). Modeling of quaternary dyes adsorption onto ZnO-NR-AC artificial neural network: Analysis by derivative spectrophotometry. *Journal of Industrial and Engineering Chemistry*, **34**: 186-197.
- Ghaedi, M., Ghayedi, M., Kokhdan, S.N., Sahraei, R. and A. Daneshfar (2013). Palladium, silver, and zinc oxide nanoparticles loaded on activated carbon as adsorbent for removal of bromophenol red from aqueous solution. *Journal of Industrial and Engineering Chemistry*, **19(4)**: 1209-1217.
- Hosseinazadeh, S., Hosseinazadeh, H., Pashaei, S. and Z. Khodaparast (2018). Synthesis of magnetic functionalized MWCNT nanocomposite through surface RAFT copolymerization of acrylic acid and N-isopropyl acrylamide for removal of cationic dyes from aqueous solutions. *Ecotoxicology and Environmental Safety*, **161**: 34-44.
- Kalantary, R.R., Farzadkia, M., Kermani, M. and M. Rahmatinia (2018). Heterogeneous electro-Fenton process by Nano-Fe<sub>3</sub>O<sub>4</sub> for catalytic degradation of amoxicillin: Process optimization using response surface methodology. *Journal of Environmental Chemical Engineering*, **6(4)**: 4644-4652.
- Karimi, R., Yousefi, F., Ghaedi, M. and Z. Rezaee (2019). Comparison the behavior of ZnO-NP-AC and Na, K doped ZnO-NP-AC for simultaneous removal of crystal violet and quinoline yellow dyes: Modeling and optimization. *Polyhedron*, **170**: 60-69.
- Khedaer, Z., Ahmed, D.S. and S.M.H. Al-Jawad (2021). Investigation of morphological, optical, and antibacterial properties of hybrid ZnO-MWCNT prepared by sol-gel. *Journal of Applied Sciences and Nanotechnology*, **1(2)**: 66-77.
- Konicki, W., Pelech, I., Mijowska, E. and I. Jasińska (2012). Adsorption of anionic dye Direct Red 23 onto magnetic multi-walled carbon nanotubes-Fe<sub>3</sub>C nanocomposite: Kinetics, equilibrium and thermodynamics. *Chemical Engineering Journal*, **210**: 87-95.
- Langmuir, I. (1918). The adsorption of gases on plane

- surfaces of glass, mica and platinum. *Journal of the American Chemical Society*, **40(9)**: 1361-1403.
- Leudjo Taka, A., Fosso-Kankeu, E., Pillay, K. and X. Yangkou Mbiand (2020). Metal nanoparticles decorated phosphorylated carbon nanotube/cyclodextrin nanosponge for trichloroethylene and Congo red dye adsorption from wastewater. *Journal of Environmental Chemical Engineering*, **8**: 103602.
- Mashkour, M.S., Al-Kaim, A.F., Ahmed, L.M. and F.H. Hussein (2011). Zinc oxide assisted photocatalytic decolorization of reactive red 2 dye. *International Journal of Chemical Sciences*, **9(3)**: 969-979.
- Mosaa, Z. A., Bader, A.T., Aljeboree, A.M. and A.F. Alkaim (2019). Adsorption and removal of textile dye (methylene blue MB) from aqueous solution by activated carbon as a model (apricot stone source waste) of plant role in environmental enhancement. *Plant Archives*, **19**: 910-914.
- Pashaei-Fakhri, S., Peighambaroust, S.J., Rauf Foroutan, R., Arsalani, N. and B. Ramavandi (2021). Crystal violet dye sorption over acrylamide/graphene oxide bonded sodium alginate nanocomposite hydrogel. *Chemosphere*, **270**: 129419.
- Radia, N.D., Kamona, S.M.H., Jasem, H., Abass, R.R., Izzat, S.E., Ali, M.S., Ghafel, S.T. and A.M. Aljeboree (2022). Role of hydrogel and study of its high-efficiency to removal streptomycin drug from aqueous solutions. *International Journal of Pharmaceutical Quality Assurance*, **13(2)**: 160-163.
- Radia, N.D., Mahdi, A.B., Mohammed, G.A., Sajid, A., Altimari, U.S., Shams, M.A., Aljeboree, A.M. and F.H. Abdulrazzak (2022). Removal of rose bengal dye from aqueous solution using low cost (SA-g-PAAc) hydrogel: Equilibrium and kinetic study. *International Journal of Drug Delivery Technology*, **12(3)**: 957-960.
- Shaw, R., Mittal, T., Tiwari, S. and S.K. Tiwari (2018). Enhanced adsorption at ZnO nanoflakes@ zeolite core shell interface: A study of changing adsorption dynamics. *Journal of Environmental Chemical Engineering*, **6(1)**: 1424-1433.
- Somu, P. and S. Paul (2018). Casein based biogenic-synthesized zinc oxide nanoparticles simultaneously decontaminate heavy metals, dyes, and pathogenic microbes: A rational strategy for wastewater treatment. *Journal of Chemical Technology & Biotechnology*, **93(10)**: 2962-2976.
- Stefaniuk, I., Cieniek, B. and I. Rogalska (2019). Magnetic properties of ZnO:Co layers obtained by pulsed laser deposition method. *Mater Sci-Pol*, **36(3)**: 439-444.
- Wared, S.H.H. and N.D. Radia (2021). Synthesis and characterization of sodium alginate-g-polyacrylic acid hydrogel and its application for crystal violet dye adsorption. *International Journal of Drug Delivery Technology*, **11(2)**: 556-565.
- Zhang, M., Chang, L. and Y. Zhao (2019). Fabrication of zinc oxide/polypyrrole nanocomposites for brilliant green removal from aqueous phase. *Arabian J. Sci. Eng.*, **44(1)**: 111-121.
- Zhao, S., Zhan, Y., Wan, X., He, S., Yang, X., Hu, J. and G. Zhang (2020). Selective and efficient adsorption of anionic dyes by core/shell magnetic MWCNTs nano-hybrid constructed through facial polydopamine tailored graft polymerization: Insight of adsorption mechanism, kinetic, isotherm and thermodynamic study. *Journal of Molecular Liquids*, **319**: 114289.

## Contents

<i>Editorial</i>	i
❑ <i>Snapshots</i>	ii
Effect of Phytoremediation of <i>Eichornia crassipes</i> (Mart.) Solms and <i>Marsilea crenata</i> C. Persl on Reduction of Phosphate Levels in Laundry Waste <i>V.N. Vatmawati and F. Rachmadiarti</i>	1
Optimisation of Reverse-Osmosis Water Purification Plant Powered by Hydro-Generators at the Dead Sea <i>Hazem W. Marar</i>	9
The High Lead Level Role in the DNA Repair RAD 18 and OGG1 Gene Polymorphism in Gasoline Station Workers <i>Aizhar Hamzih Hasan, Dhuha Salman Asker Aljuboory, Hawraa Hamid Hussein and Mona N. Al-Terehi</i>	17
Cost-Effective Utilisation of Industrial Fly Ash Waste in Treatment of Domestic Wastewater <i>Subhakanta Dash, Itishree Mohanty, Rudra Prasanna Nayak, Piyush Gupta, Saroj Barik and Laxmidhar Panda</i>	23
Vermicompost, Phosphorous Nano-Fertiliser and Humic Acid: Their Effect on the Activity of Inorganic Pyrophosphatase Enzyme and its Thermodynamic Parameters <i>Luma Salih Jabbar Al-Taweel and Ahmed Malik Waheed AlSaadawi</i>	31
Exposure of Ambient PM <sub>2.5</sub> and Acute Upper-and Lower Respiratory Infection in Children Under the Age of Five in South and Southeast Asia <i>Made Ayu Hitapretiwi Suryadhi, Kawuli Abudureyimu, Ni Komang Ekawati, I Made Winarsa Ruma, Putu Ayu Rhamani Suryadhi and Takashi Yorifuji</i>	41
Biosorption of Pollutants in Diyala River by Using Irrigated Vegetables <i>Haider A.J. Almuslamawy, Rasha Ahmed Hashim, Ahmed Hussein Ali Aldhrub and Raghad S. Mouhamad</i>	51
A Combined Approach for the Treatment of Textile Dye Bath Effluent Using CO <sub>2</sub> Gas <i>Venkatesan Govindaraj, Kalpana Manoharan, Sakthivel S., Guruchandran K. and Mathew W.</i>	59
Water Birds Diversity Variations in Tidal and Non-tidal Wetland Habitats in East Al_Hammar Marsh South of Iraq <i>Aqeel Laftah Al-Emarah and Mufid Kassim Abou-Turab</i>	67
Estimation of Air Pollutants Along with Meteorological Parameters and Study of Their Impact on Human Health <i>Mehraj Uddin Bhat, Anish C. Pandey and Mohd Aadil Deva</i>	75
Carbon Capture and Storage with Ionic Liquids: Industrial Flue Gas Trapping in Calcination Process <i>Venkatesan Govindaraj, Kuberan Murugan, Jegadeesh Sathaiya and Praveen Baskar</i>	85
Evaluation of the Effects of Riparian Population Activities on the Physicochemical Quality of Water in a Mediterranean River: The Inaouene River (Taza, North East Morocco) <i>F.E. Sghiouer, A. Nahli, H. Bouka and M. Chlaida</i>	93
Environment News Futures	101